Learning to Simulate Dynamic Environments with GameGAN

Seung Wook Kim[1,2,3*]   Yuhao Zhou[2†]   Jonah Philion[1,2,3]   Antonio Torralba[4]   Sanja Fidler[1,2,3*]

[1]NVIDIA   [2]University of Toronto   [3]Vector Institute   [4] MIT

{seungwookk,jphilion,sfidler}@nvidia.com   henryzhou@cs.toronto.edu   torralba@mit.edu

https://nv-tlabs.github.io/gameGAN

Abstract

Simulation is a crucial component of any robotic system. In order to simulate correctly, we need to write complex rules of the environment: how dynamic agents behave, and how the actions of each of the agents affect the behavior of others. In this paper, we aim to learn *a simulator by simply watching an agent interact with an environment. We focus on graphics games as a proxy of the real environment. We introduce GameGAN, a generative model that learns to visually imitate a desired game by ingesting screenplay and keyboard actions during training. Given a key pressed by the agent, GameGAN "renders" the next screen using a carefully designed generative adversarial network. Our approach offers key advantages over existing work: we design a memory module that builds an internal map of the environment, allowing for the agent to return to previously visited locations with high visual consistency. In addition, GameGAN is able to disentangle static and dynamic components within an image making the behavior of the model more interpretable, and relevant for downstream tasks that require explicit reasoning over dynamic elements. This enables many interesting applications such as swapping different components of the game to build new games that do not exist.*

1. Introduction

Before deployment to the real world, an artificial agent needs to undergo extensive testing in challenging simulated environments. Designing good simulators is thus extremely important. This is traditionally done by writing procedural models to generate valid and diverse scenes, and complex behavior trees that specify how each actor in the scene behaves and reacts to actions made by other actors, including the ego agent. However, writing simulators that encompass a large number of diverse scenarios is extremely time consuming and requires highly skilled graphics experts. Learn-
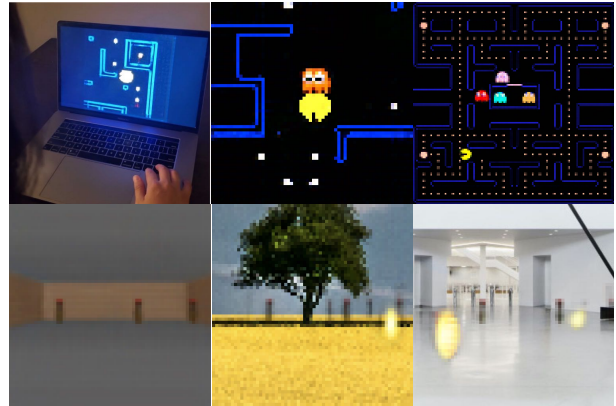

Figure 1: If you look at the person on the top-left picture, you might think she is playing Pacman of Toru Iwatani, but she is not! She is actually playing with a GAN generated version of Pacman. In this paper, we introduce GameGAN that learns to reproduce games by just observing lots of playing rounds. Moreover, our model can disentangle background from dynamic objects, allowing us to create new games by swapping components as shown in the center and right images of the bottom row.

ing to simulate by simply observing the dynamics of the real world is the most scaleable way going forward.

A plethora of existing work aims at learning behavior models [2, 33, 19, 4]. However, these typically assume a significant amount of supervision such as access to agents' ground-truth trajectories. We aim to learn a simulator by simply watching an agent interact with an environment. To simplify the problem, we frame this as a 2D image generation problem. Given sequences of observed image frames and the corresponding actions the agent took, we wish to emulate image creation as if "rendered" from a real dynamic environment that is reacting to the agent's actions.

Towards this goal, we focus on graphics games, which represent simpler and more controlled environments, as a proxy of the real environment. Our goal is to replace the graphics engine at test time, by visually imitating the game using a learned model. This is a challenging problem: different games have different number of components as well as different physical dynamics. Furthermore, many games require long-term consistency in the environment. For example, imagine a game where an agent navigates through a
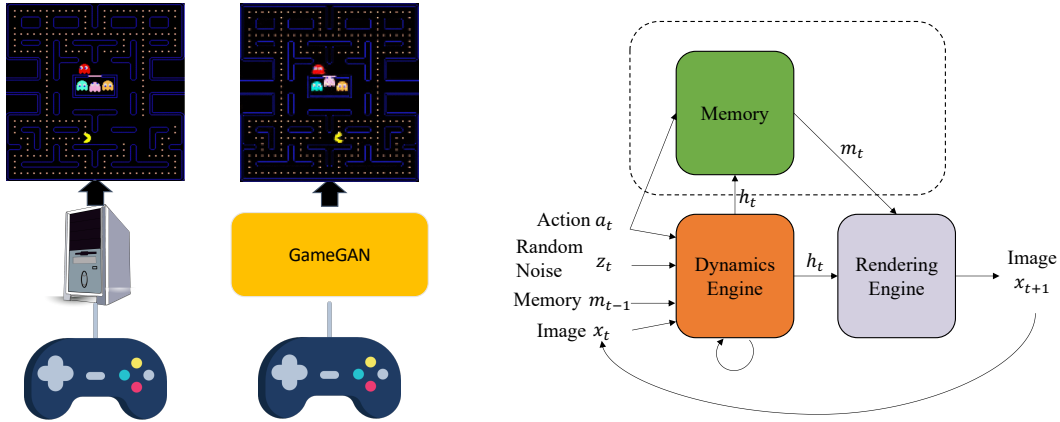

Figure 2: Overview of GameGAN: Our goal is to replace the game engine with neural networks. GameGAN is composed of three main modules. The *dynamics engine* is implemented as an RNN, and contains the world state that is updated at each time t. Optionally, it can write to and read from the external *memory module* $\mathcal{M}$. Finally, the *rendering engine* is used to decode the output image. All modules are neural networks and trained end-to-end.

maze. When the agent moves away and later returns to a location, it expects the scene to look consistent with what it has encountered before. In visual SLAM, *detecting* loop closure (returning to a previous location) is already known to be challenging, let alone *generating* one. Last but not least, both deterministic and stochastic behaviors typically exist in a game, and modeling the latter is known to be particularly hard.

In this paper, we introduce GameGAN, a generative model that learns to imitate a desired game. GameGAN ingests screenplay and keyboard actions during training and aims to predict the next frame by conditioning on the action, *i.e.* a key pressed by the agent. It learns from rollouts of image and action pairs directly without having access to the underlying game logic or engine. We make several advancements over the recently introduced World Model [13] that aims to solve a similar problem. By leveraging Generative Adversarial Networks [10], we produce higher quality results. Moreover, while [13] employs a straightforward conditional decoder, GameGAN features a carefully designed architecture. In particular, we propose a new memory module that encourages the model to build an internal map of the environment, allowing the agent to return to previously visited locations with high visual consistency. Furthermore, we introduce a purposely designed decoder that learns to disentangle static and dynamic components within the image. This makes the behavior of the model more interpretable, and it further allows us to modify existing games by swapping out different components.

We test GameGAN on a modified version of Pacman and the VizDoom environment [20], and propose several synthetic tasks for both quantitative and qualitative evaluation. We further introduce a come-back-home task to test the long-term consistency of learned simulators. Note that GameGAN supports several applications such as transferring a given game from one operating system to the other,

without requiring to re-write code.

2. Related Work

Generative Adversarial Networks: In GANs [10], a generator and a discriminator play an adversarial game that encourages the generator to produce realistic outputs. To obtain a desired control over the generated outputs, categorical labels [28], images [18, 25], captions [34], or masks [32] are provided as input to the generator. Works such as [39] synthesize new videos by transferring the style of the source to the target video using the cycle consistency loss [41, 21]. Note that this is a simpler problem than the problem considered in our work, as the dynamic content of the target video is provided and only the visual style needs to be modified. In this paper, we consider generating the dynamic content itself. We adopt the GAN framework and use the user-provided action as a condition for generating future frames. To the best of our knowledge, ours is the first work on using action-conditioned GANs for emulating game simulators.

Video Prediction: Our work shares similarity to the task of video prediction which aims at predicting future frames given a sequence of previous frames. Several works [36, 6, 31] train a recurrent encoder to decode future frames. Most approaches are trained with a reconstruction loss, resulting in a deterministic process that generates blurry frames and often does not handle stochastic behaviors well. The errors typically accumulate over time and result in low quality predictions. Action-LSTM models [6, 31] achieved success in scaling the generated images to higher resolution but do not handle complex stochasticity present in environments like Pacman. Recently, [13, 8] proposed VAE-based frameworks to capture the stochasticity of the task. However, the resulting videos are blurry and the generated frames tend to omit certain details. GAN loss has been previously used in several works [9, 24, 37, 7]. [9] uses an adversarial loss to
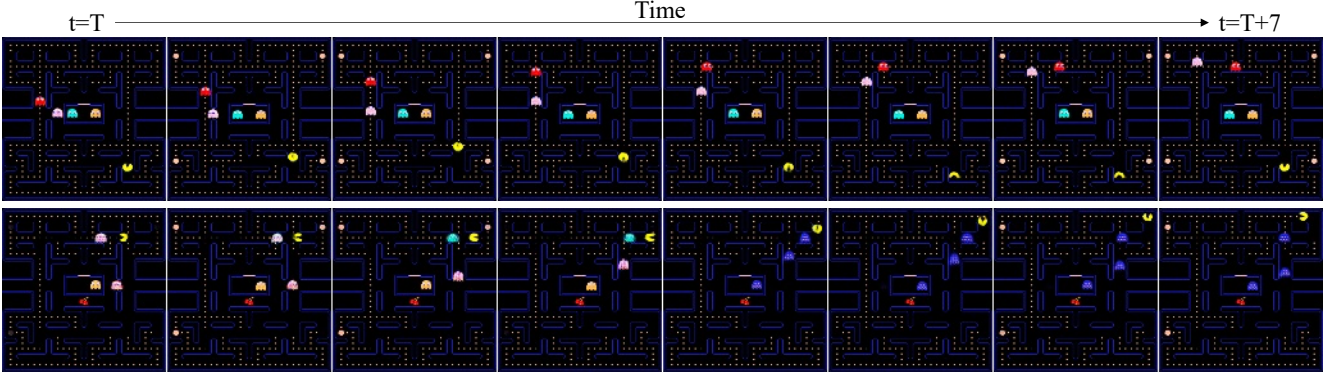
Figure 3: Screenshots of a human playing with GameGAN trained on the official version of Pac-Man[1]. GameGAN learns to produce a visually consistent simulation as well as learning the dynamics of the game well. On the bottom row, the player consumes a capsule, turning the ghosts purple. Note that ghosts approach Pacman before consuming the capsule, and run away after.

disentangle pose from content across different videos. In [24], VAE-GAN [23] formulation is used for generating the next frame of the video. Our model differs from these works in that in addition to generating the next frame, GameGAN also learns the intrinsic dynamics of the environment. [12] learns a game engine by parsing frames and learning a rule-based search engine that finds the most likely next frame. GameGAN goes one step further by learning everything from frames and also learning to directly generate frames.

World Models: In model-based reinforcement learning, one uses interaction with the environment to learn a dynamics model. World Models [13] exploit a learned simulated environment to train an RL agent instead. Recently, World Models have been used to generate Atari games in a concurrent work [1]. The key differences with respect to these models are in the design of the architecture: we introduce a memory module to better capture long-term consistency, and a carefully designed decoder that disentangles static and dynamic components of the game.

3. GameGAN

We are interested in training a game simulator that can model both deterministic and stochastic nature of the environment. In particular, we focus on an action-conditioned simulator in the image space where there is an egocentric agent that moves according to the given action $a_t \sim \mathcal{A}$ at time t and generates a new observation x_{t+1}. We assume there is also a stochastic variable $z_t \sim \mathcal{N}(0; I)$ that corresponds to randomness in the environment. Given the history of images $x_{1:t}$ along with a_t and z_t, GameGAN predicts the next image x_{t+1}. GameGAN is composed of three main modules. The *dynamics engine* (Sec 3.1), which maintains an internal state variable, takes a_t and z_t as inputs and updates the current state. For environments that require long-

term consistency, we can optionally use an external *memory module* (Sec 3.2). Finally, the *rendering engine* (Sec 3.3) produces the output image given the state of the dynamics engine. It can be implemented as a simple convolutional decoder or can be coupled with the memory module to disentangle static and dynamic elements while ensuring long-term consistency. We use adversarial losses along with a proposed temporal cycle loss (Sec 3.4) to train GameGAN. Unlike some works [13] that use sequential training for stability, GameGAN is trained end-to-end. We provide more details of each module in the supplementary materials.

3.1. Dynamics Engine

GameGAN has to learn how various aspects of an environment change with respect to the given user action. For instance, it needs to learn that certain actions are not possible (*e.g.* walking through a wall), and how other objects behave as a consequence of the action. We call the primary component that learns such transitions the *dynamics engine* (see illustration in Figure 2). It needs to have access to the past history to produce a consistent simulation. Therefore, we choose to implement it as an action-conditioned LSTM [15], motivated by the design of Chiappa *et al.* [6]:

$$v_t = h_{t-1} \odot \mathcal{H}(a_t, z_t, m_{t-1}), s_t = \mathcal{C}(x_t) \quad (1)$$

$$i_t = \sigma(W^{iv}v_t + W^{is}s_t), f_t = \sigma(W^{fv}v_t + W^{fs}s_t), \quad (2)$$
$$o_t = \sigma(W^{ov}v_t + W^{os}s_t)$$

$$c_t = f_t \odot c_{t-1} + i_t \odot \tanh(W^{cv}v_t + W^{cs}s_t) \quad (3)$$

$$h_t = o_t \odot \tanh(c_t) \quad (4)$$

where h_t, a_t, z_t, c_t, x_t are the hidden state, action, stochastic variable, cell state, image at time step t. m_{t-1} is the retrieved memory vector in the previous step (if the memory module is used), and i_t, f_t, o_t are the input, forget, and output gates. a_t, z_t, m_{t-1} and h_t are fused into v_t, and s_t is
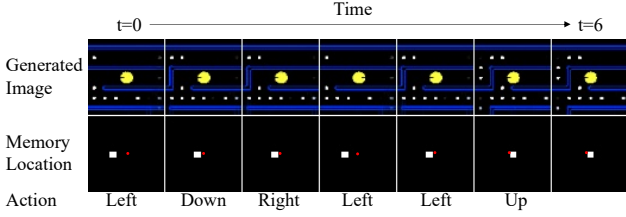
Figure 4: Visualizing attended memory location α: Red dots marking the center are placed to aid visualization. Note that we *learn* the memory shift, so the user action does not always align with how the memory is shifted. In this case, *Right* shifts α to the left, and *Left* shifts α to the right. It also *learns* not to shift when an invalid action is given.

the encoding of the image x_t. $\mathcal{H}$ is a MLP, $\mathcal{C}$ is a convolutional encoder, and W are weight matrices. $\odot$ denotes the hadamard product. The engine maintains the standard state variables for LSTM, h_t and c_t, which contain information about every aspect of the current environment at time t. It computes the state variables given a_t, z_t, m_{t-1}, and x_t.

3.2. Memory Module

Suppose we are interested in simulating an environment in which there is an agent navigating through it. This requires long-term consistency in which the simulated scene (*e.g.* buildings, streets) should not change when the agent comes back to the same location a few moments later. This is a challenging task for typical models such as RNNs because 1) the model needs to remember every scene it generates in the hidden state, and 2) it is non-trivial to design a loss that enforces such long-term consistency. We propose to use an external memory module, motivated by the Neural Turing Machine (NTM) [11].

The memory module has a memory block $\mathcal{M} \in \mathbb{R}^{N \times N \times D}$, and the attended location $\alpha_t \in \mathbb{R}^{N \times N}$ at time t. $\mathcal{M}$ contains $N \times N$ D-dimensional vectors where N is the spatial width and height of the block. Intuitively, α_t is the current location that the egocentric agent is located at. $\mathcal{M}$ is initialized with random noise $\sim N(0, I)$ and α_0 is initialized with 0s except for the center location $(N/2, N/2)$ that is set to 1. At each time step, the memory module computes:

$$w = \text{softmax}(\mathcal{K}(a_t)) \in \mathbb{R}^{3 \times 3} \quad (5)$$

$$g = \mathcal{G}(h_t) \in \mathbb{R} \quad (6)$$

$$\alpha_t = g \cdot \text{Conv2D}(\alpha_{t-1}, w) + (1 - g) \cdot \alpha_{t-1} \quad (7)$$

$$\mathcal{M} = \text{write}(\alpha_t, \mathcal{E}(h_t), \mathcal{M}) \quad (8)$$

$$m_t = \text{read}(\alpha_t, \mathcal{M}) \quad (9)$$

where $\mathcal{K}$, $\mathcal{G}$ and $\mathcal{E}$ are small MLPs. w is a learned shift kernel that depends on the current action, and the kernel is used to shift α_{t-1}. In some cases, the shift should not happen (*e.g.* cannot go forward at a dead end). With the help from h_t, we also learn a gating variable $g \in [0, 1]$ that determines if α should be shifted or not. $\mathcal{E}$ is learned to extract information to be written from the hidden state. Finally, $write$ and
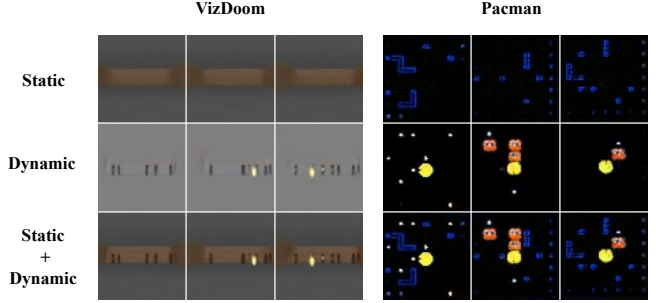

Figure 5: Example showing how static and dynamic elements are disentangled in VizDoom and Pacman games with GameGAN . Static components usually include environmental objects such as walls. Dynamic elements typically are objects that can change as the game progresses such as food and other non-player characters.

$read$ operations softly access the memory location specified by α similar to other neural memory modules [11]. Using this shift-based memory module allows the model to not be bounded by the block $\mathcal{M}$'s size while enforcing local movements. Therefore, we can use any arbitrarily sized block at test time. Figure 4 demonstrates the learned memory shift. Since the model is free to assign actions to different kernels, the learned shift does not always correspond to how humans would do. We can see that *Right* is assigned as a left-shift, and hence *Left* is assigned as a right-shift. Using the gating variable g, it also learns not to shift when an invalid action, such as going through a wall, is given.

Enforcing long-term consistency in our case refers to remembering generated static elements (*e.g.* background) and retrieving them appropriately when needed. Accordingly, the benefit of using the memory module would come from storing static information inside it. Along with a novel cycle loss (Section 3.4.2), we introduce inductive bias in the architecture of the rendering engine (Section 3.3) to encourage the disentanglement of static and dynamic elements.

3.3. Rendering Engine

The (neural) *rendering engine* is responsible for rendering the simulated image x_{t+1} given the state h_t. It can be simply implemented with standard transposed convolution layers. However, we also introduce a specialized rendering engine architecture (Figure 6) for ensuring long-term consistency by learning to produce disentangled scenes. In Section 4, we compare the benefits of each architecture.

The specialized rendering engine takes a list of vectors $\mathbf{c} = \{c^1, ..., c^K\}$ as input. In this work, we let $K = 2$, and $\mathbf{c} = \{m_t, h_t\}$. Each vector c^k corresponds to one type of entity and goes through the following three stages (see Fig 6). First, c^k is fed into convolutional networks to produce an attribute map $A^k \in \mathbb{R}^{H_1 \times H_1 \times D_1}$ and object map $O^k \in \mathbb{R}^{H_1 \times H_1 \times 1}$. It is also fed into a linear layer to get the type vector $v^k \in \mathbb{R}^{D_1}$ for the k-th component. O for all components are concatenated together and fed through
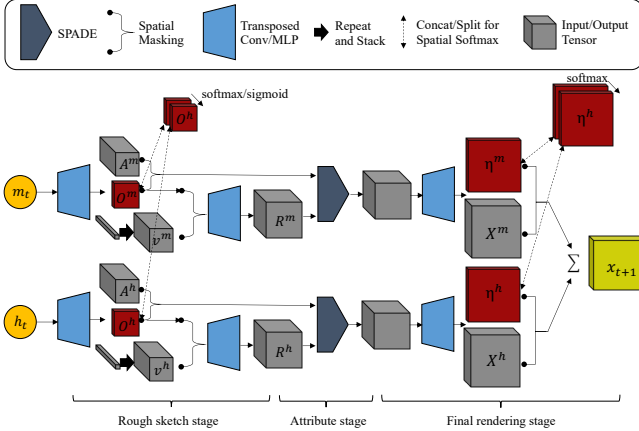
Figure 6: *Rendering engine* for disentangling static and dynamic components. See Sec 3.3 for details.

either a sigmoid to ensure $0 \leq O^k[x][y] \leq 1$ or a spatial softmax function so that $\sum_{k=1}^{K} O^k[x][y] = 1$ for all x, y. The resulting object map is multiplied by the type vector v^k in every location and fed into a convnet to produce $R^k \in \mathbb{R}^{H_2 \times H_2 \times D_2}$. This is a rough sketch of the locations where k-th type objects are placed. However, each object could have different attributes such as different style or color. Hence, it goes through the attribute stage where the tensor is transformed by a SPADE layer [32, 16] with the masked attribute map $O^k \odot A^k$ given as the contextual information. It is further fed through a few transposed convolution layers, and finally goes through an attention process similar to the rough sketch stage where concatenated components goes through a spatial softmax to get fine masks. The intuition is that after drawing individual objects, it needs to decide the "depth" ordering of the objects to be drawn in order to account for occlusions. Let us denote the fine mask as η^k and the final tensor as X^k. After this process, the final image is obtained by summing up all components, $x = \sum_{k=1}^{K} \eta^k \odot X^k$. Therefore, the architecture of our neural rendering engine encourages it to extract different information from the memory vector and the hidden state with the help of temporal cycle loss (Section 3.4.2). We also introduce a version with more capacity that can produce higher quality images in Section A.5 of the supplementary materials.

3.4. Training GameGAN

Adversarial training has been successfully employed for image and video synthesis tasks. GameGAN leverages adversarial training to learn environment dynamics and to produce realistic temporally coherent simulations. For certain cases where long-term consistency is required, we propose temporal cycle loss that disentangles static and dynamic components to learn to remember what it has generated.

3.4.1 Adversarial Losses

There are three main components: single image discriminator, action discriminator, and temporal discriminator.

Single image discriminator: To ensure each generated frame is realistic, the single image discriminator and GameGAN simulator play an adversarial game.

Action-conditioned discriminator: GameGAN has to reflect the actions taken by the agent faithfully. We give three pairs to the action-conditioned discriminator: (x_t, x_{t+1}, a_t), $(x_t, x_{t+1}, \bar{a}_t)$ and $(\hat{x}_t, \hat{x}_{t+1}, a_t)$. x_t denotes the real image, $\hat{x}_t$ the generated image, and $\bar{a}_t \in \mathcal{A}$ a sampled negative action $\bar{a}_t \neq a_t$. The job of the discriminator is to judge if two frames are consistent with respect to the action. Therefore, to fool the discriminator, GameGAN has to produce realistic future frame that reflects the action.

Temporal discriminator: Different entities in an environment can exhibit different behaviors, and also appear or disappear in partially observed states. To simulate a temporally consistent environment, one has to take past information into account when generating the next states. Therefore, we employ a temporal discriminator that is implemented as 3D convolution networks. It takes several frames as input and decides if they are a real or generated sequence.

Since conditional GAN architectures [27] are known for learning simplified distributions ignoring the latent code [40, 35], we add information regularization [5] that maximizes the mutual information $I(z_t, \phi(x_t, x_{t+1}))$ between the latent code z_t and the pair (x_t, x_{t+1}). To help the action-conditioned discriminator, we add a term that minimizes the cross entropy loss between a_t and $a_t^{pred} = \psi(x_{t+1}, x_t)$. Both ϕ and ψ are MLP that share layers with the action-conditioned discriminator except for the last layer. Lastly, we found adding a small reconstruction loss in image and feature spaces helps stabilize the training (for feature space, we reduce the distance between the generated and real frame's single image discriminator features). A detailed descriptions are provided in the supplementary material.

3.4.2 Cycle Loss

RNN based generators are capable of keeping track of the recent past to generate coherent frames. However, it quickly forgets what happened in the distant past since it is encouraged simply to produce realistic next observation. To ensure long-term consistency of static elements, we leverage the memory module and the rendering engine to disentangle static elements from dynamic elements.

After running through some time steps T, the memory block $\mathcal{M}$ is populated with information from the dynamics engine. Using the memory location history α_t, we can retrieve the memory vector $\hat{m}_t$ which could be different from m_t if the content at the location α_t has been modified. Now, $c = \{\hat{m}_t, \mathbf{0}\}$ is passed to the rendering engine to produce
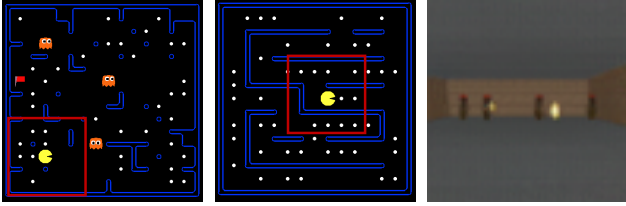
Figure 7: Samples from datasets studied in this work. For Pacman and Pacman-Maze, training data consists of partially observed states, shown in the red box. Left: Pacman, Center: Pacman-Maze, Right: VizDoom

$X^{\hat{m}_t}$ where $\mathbf{0}$ is the zero vector and $X^{\hat{m}_t}$ is the output component corresponding to $\hat{m}_t$. We use the following loss:

$$L_{cycle} = \sum_t^T ||X^{m_t} - X^{\hat{m}_t}|| \qquad (10)$$

As dynamic elements (*e.g.* moving ghosts in Pacman) do not stay the same across time, the engine is encouraged to put static elements in the memory vector to reduce L_{cycle}. Therefore, long-term consistency is achieved.

To prevent the trivial solution where the model tries to ignore the memory component, we use a regularizer that minimizes the sum of all locations in the fine mask $\min \sum \eta^h$ from the hidden state vector so that X^{m_t} has to contain content. Another trivial solution is if shift kernels for all actions are learned to never be in the opposite direction of each other. In this case, $\hat{m}_t$ and m_t would always be the same because the same memory location will never be revisited. Therefore, we put a constraint that for actions a with a negative counterpart $\hat{a}$ (*e.g. Up* and *Down*), $\hat{a}$'s shift kernel $\mathcal{K}(\hat{a})$ is equal to horizontally and vertically flipped $\mathcal{K}(a)$. Since most simulators that require long-term consistency involves navigation tasks, it is trivial to find such counterparts.

3.4.3 Training Scheme

GameGAN is trained end-to-end. We employ a warm-up phase where real frames are fed into the dynamics engine for the first few epochs, and slowly reduce the number of real frames to 1 (the initial frame x_0 is always given). We use 18 and 32 frames for training GameGAN on Pacman and VizDoom environments, respectively.

4. Experiments

We present both qualitative and quantitative experiments. We mainly consider four models: 1) Action-LSTM: model trained only with reconstruction loss which is in essence similar to [6], 2) World Model [13], 3) GameGAN-M: our model without the memory module and with the simple rendering engine, and 4) GameGAN: the full model with the memory module and the rendering engine for disentanglement. Experiments are conducted on the following three datasets (Figure 7):

Pacman: We use a modified version of the Pacman game[2] in which the Pacman agent observes an egocentric 7x7 grid from the full 14x14 environment. The environment is randomly generated for each episode. This is an ideal environment to test the quality of a simulator since it has both deterministic (*e.g.*, game rules & viewpoint shift) and highly stochastic components (*e.g.*, game layout of foods and walls; game dynamics with moving ghosts). Images in the episodes are 84x84 and the action space is $\mathcal{A} = \{left, right, up, down, stay\}$. 45K episodes of length greater than or equal to 18 are extracted and 40K are used for training. Training data is generated by using a trained DQN [30] agent that observes the full environment with high entropy to allow exploring diverse action sequences. Each episode consists of a sequence of 7x7 Pacman-centered grids along with actions.

Pacman-Maze: This game is similar to Pacman except that it does not have ghosts, and its walls are randomly generated from a maze-generation algorithm, thus are structured better. The same number of data is used as Pacman.

Vizdoom: We follow the experiment set-up of Ha and Schmidhuber [13] that uses *takecover* mode of the Viz-Doom platform [20]. Training data consists of 10k episodes extracted with random policy. Images in the episodes are 64x64 and the action space is $\mathcal{A} = \{left, right, stay\}$

4.1. Qualitative Evaluation

Figure 8 shows rollouts of different models on the Pacman dataset. Action-LSTM, which is trained only with reconstruction loss, produces blurry images as it fails to capture the multi-modal future distribution, and the errors accumulate quickly. World model [13] generates realistic images for VizDoom, but it has trouble simulating the highly stochastic Pacman environment. In particular, it sometimes suffers from large unexpected discontinuities (*e.g.* $t = 0$ to $t = 1$). On the other hand, GameGAN produces temporally consistent and realistic sharp images. GameGAN consists of only a few convolution layers to roughly match the number of parameters of World Model. We also provide a version of GameGAN that can produce higher quality images in the supplementary materials Section A.5.

Disentangling static & dynamic elements: Our GameGAN with the memory module is trained to disentangle static elements from dynamic elements. Figure 5 shows how walls from the Pacman environment and the room from the VizDoom environment are separated from dynamic objects such as ghosts and fireballs. With this, we can make interesting environments in which each element is swapped with other objects. Instead of the depressing room of Viz-Doom, enemies can be placed in the user's favorite place, or alternatively have Mario run around the room (Figure 9). We can swap the background without having to modify the
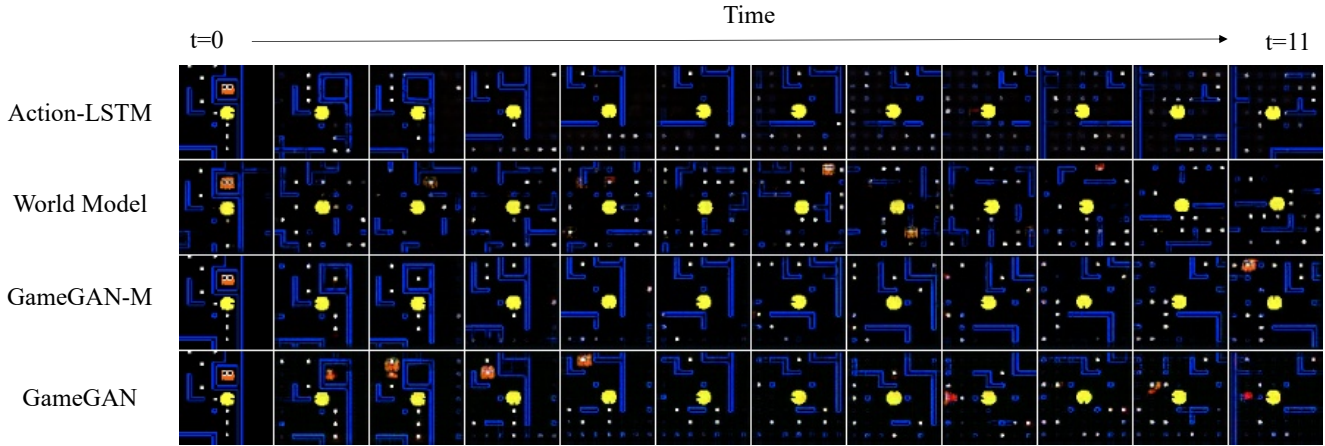
---

[2]http://ai.berkeley.edu/project_overview.html

Figure 8: Rollout of models from the same initial screen. Action-LSTM trained with reconstruction loss produces frames without refined details (*e.g.* foods). World Model has difficulty keeping temporal consistency, resulting in occasional significant discontinuities. GameGAN can produce consistent simulation.
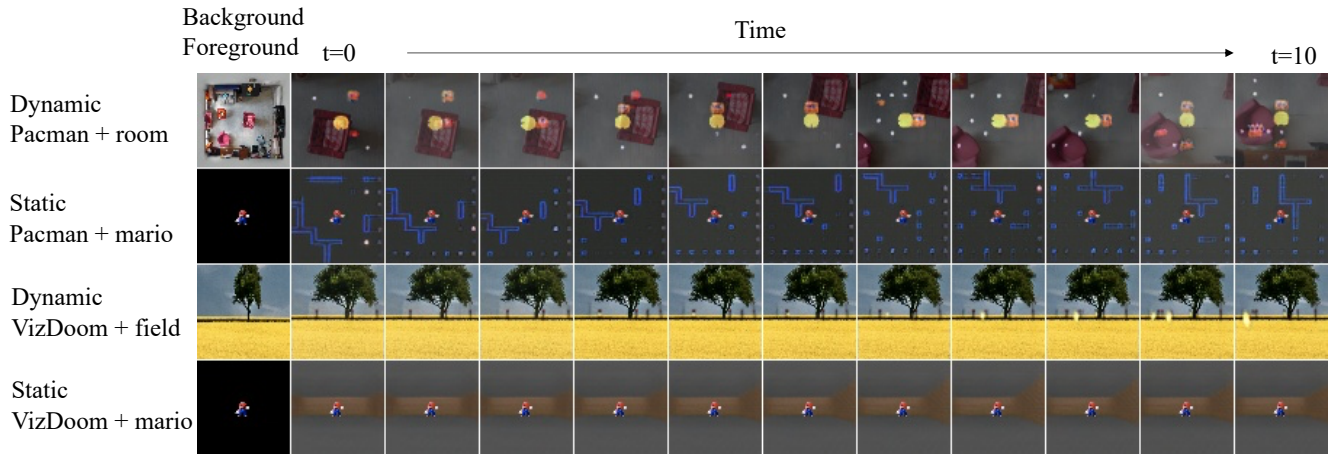

Figure 9: GameGAN on Pacman and VizDoom with swapping background/foreground with random images.
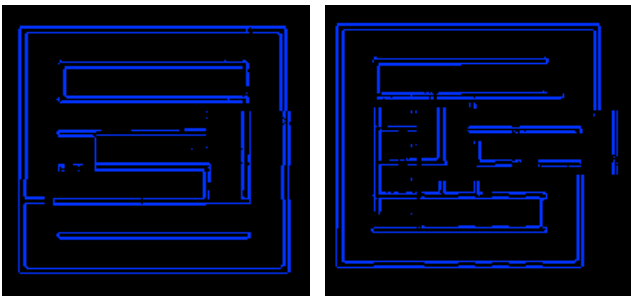

Figure 10: Generated mazes by traversing with a pacman agent on GameGAN model. Most mazes are realistic. Right shows a failure case that does not close the loop correctly.

code of the original games. Our approach treats games as a black box and learns to reproduce the game, allowing us to easily modify it. Disentangled models also open up many promising future directions that are not possible with ex-

isting models. One interesting direction would be learning multiple disentangled models and swapping certain components. As the dynamics engine learns the rules of an environment and the rendering engine learns to render images, simply learning a linear transformation from the hidden state of one model to make use of the rendering engine of the other could work.

Pacman-Maze generation: GameGAN on the Pacman-Maze produces a partial grid at each time step which can be connected to generate the full maze. It can generate realistic walls, and as the environment is sufficiently small, GameGAN also learns the rough size of the map and correctly draws the rectangular boundary in most cases. One failure case is shown in the bottom right corner of Figure 10, that fails to close the loop.

4.2. Task 1: Training an RL Agent

Quantitatively measuring environment quality is challenging as the future is multi-modal, and the ground truth
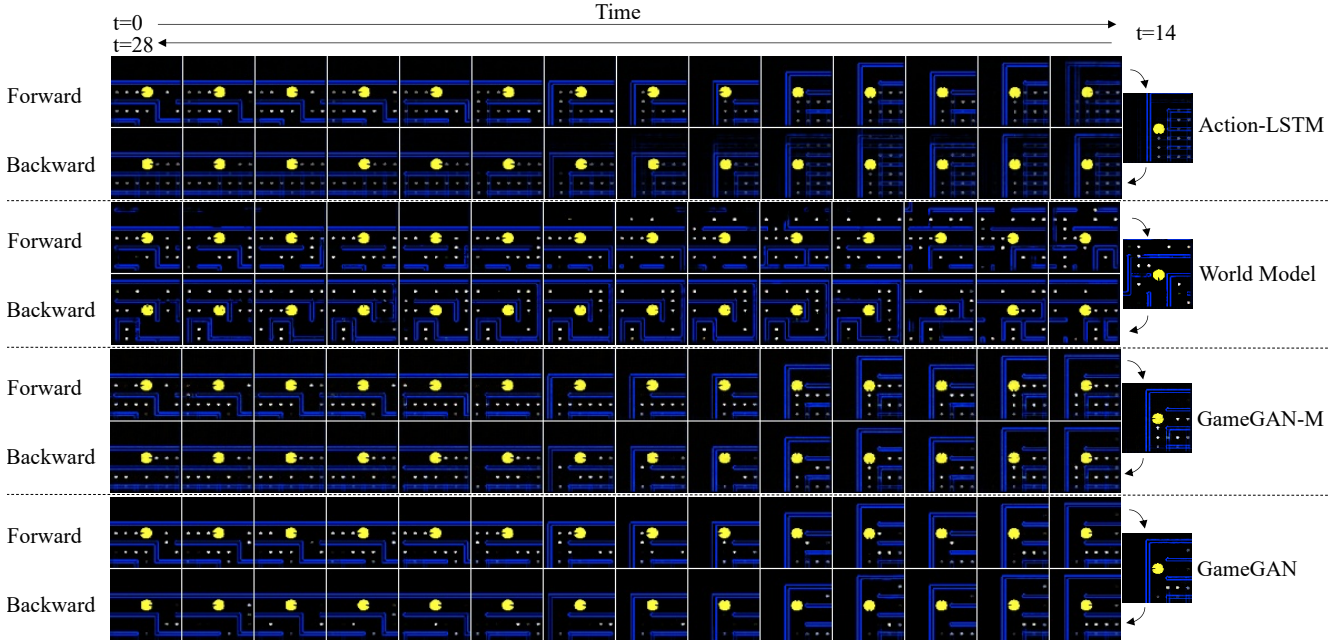
Figure 11: Come-back-home task rollouts. The forward rows show the path going from the initial position to the goal position. The backward rows show the path coming back to the initial position. Only the full GameGAN can successfully recover the initial position.
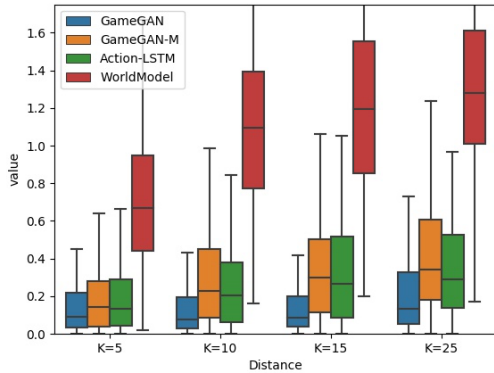

Figure 12: Box plot for Come-back-home metric. Lower is better. As a reference, a pair of randomly selected frames from the same episode gives a score of 1.17 ± 0.56

future does not exist. One way of measuring it is through learning a reinforcement learning agent inside the simulated environment and testing the trained agent in the real environment. The simulated environment should be sufficiently close to the real one to do well in the real environment. It has to learn the dynamics, rules, and stochasticity present in the real environment. The agent from the better simulator that closely resembles the real environment should score higher. We note that this is closely related to model-based RL. Since GameGAN do not internally have a mechanism for denoting the game score, we train an external classifier. The classifier is given N previous image frames and the current action to produce the output (*e.g.* Win/Lose).

Pacman: For this task, the Pacman agent has to achieve a high score by eating foods (+0.5 reward) and capturing the flag (+1 reward). It is given -1 reward when eaten by a ghost, or the maximum number of steps (40) are used. Note that this is a challenging partially-observed reinforcement learning task where the agent observes 7x7 grids. The agents are trained with A3C [29] with an LSTM component.

VizDoom: We use the Covariance Matrix Adaptation Evolution Strategy [14] to train RL agents. Following [13], we use the same setting with corresponding simulators.

	Pacman	VizDoom
Random Policy	-0.20 ± 0.78	210 ± 108
Action-LSTM[6]	-0.09 ± 0.87	280 ± 104
WorldModel[13]	1.24 ± 1.82	1092 ± 556
GameGAN $-M$	1.99 ± 2.23	724 ± 468
GameGAN	1.13 ± 1.56	765 ± 482

Table 1: Numbers are reported as mean scores ± standard deviation. Higher is better. For Pacman, an agent trained in real environment achieves 3.02 ± 2.64 which can be regarded as the upper bound. VizDoom is considered solved when a score of 750 is achieved.

Table 1 shows the results. For all experiments, scores are calculated over 100 test environments, and we report the mean scores along with standard deviation. Agents trained in Action-LSTM simulator performs similar to the agents with random policy, indicating the simulations are far from the real ones. On Pacman, GameGAN-M shows the best
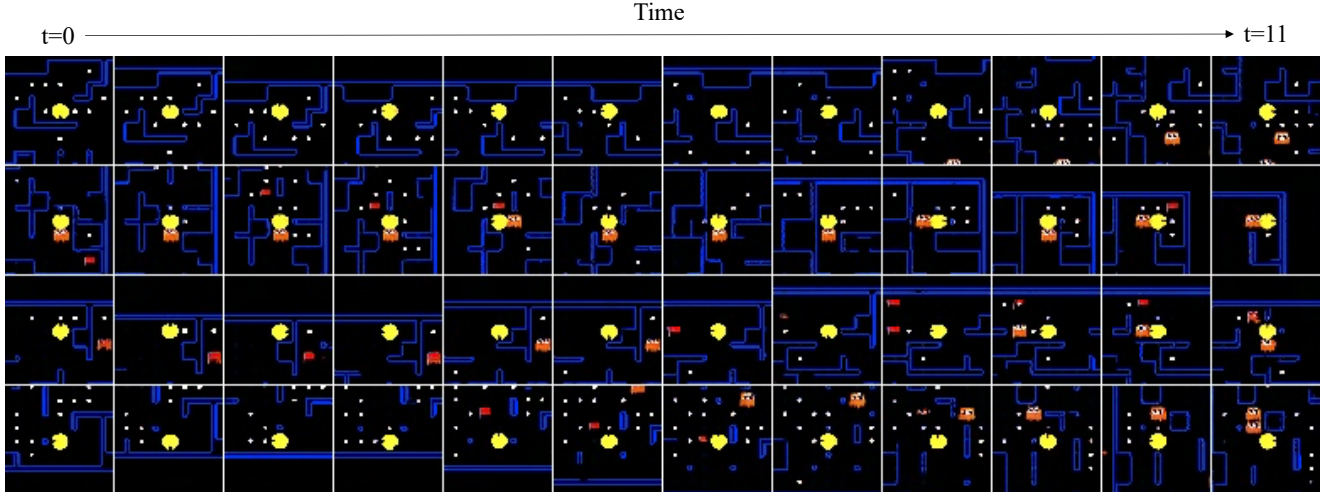
Figure 13: Pacman rollouts with a higher-capacity GameGAN described in Section A.5. The image quality is visibly better than the simpler GameGAN model shown in Figure 8.

performance while GameGAN and WorldModel have similar scores. VizDoom is considered solved when a score of 750 is achieved, and GameGAN solves the game. Note that World Model achieves a higher score, but GameGAN is the first work trained with a GAN framework that solves the game. Moreover, GameGAN can be trained end-to-end, unlike World Model that employs sequential training for stability. One interesting observation is that GameGAN shows lower performance than GameGAN-M on the Pacman environment. This is due to having additional complexity in training the model where the environments do not need long-term consistency for higher scores. We found that optimizing the GAN objective while training the memory module was harder, and this attributes to RL agents exploiting the imperfections of the environments to find a way to cheat. In this case, we found that GameGAN sometimes failed to prevent agents from walking through the walls while GameGAN-M was nearly perfect. This led to RL agents discovering a policy that liked to hit the walls, and in the real environment, this often leads to premature death. In the next section, we show how having long-term consistency can help in certain scenarios.

4.3. Task 2: Come-back-home

This task evaluates the long-term consistency of simulators in the Pacman-Maze environment. The Pacman starts at a random initial position (x_A, y_A) with state s. It is given K random actions $(a_1, ..., a_K)$, ending up in position (x_B, y_B). Using the reverse actions $(\hat{a}_K, ..., \hat{a}_1)$(*e.g.* $a_k = Down, \hat{a}_k = Up$), it comes back to the initial position (x_A, y_A), resulting in state $\hat{s}$. Now, we can measure the distance d between $\hat{s}$ and s to evaluate long-term consistency ($d = 0$ for the real environment). As elements other

than the wall (*e.g.* food) could change, we only compare the walls of $\hat{s}$ and s. Hence, s is an 84x84 binary image whose pixel is 1 if the pixel is blue. We define the metric d as

$$d = \frac{\text{sum}(\text{abs}(s - \hat{s}))}{\text{sum}(s) + 1} \qquad (11)$$

where $\text{sum}()$ counts the number of 1s. Therefore, d measures the ratio of the number of pixels changed to the initial number of pixels. Figure 12 shows the results. We again observe occasional large discontinuities in World Model that hurts the performance a lot. When K is small, the differences in performance are relatively small. This is because other models also have short-term consistency realized through RNNs. However, as K becomes larger, GameGAN with memory module steadily outperforms other models, and the gaps become larger, indicating GameGAN can make efficient use of the memory module. Figure 11 shows the rollouts of different models in the Pacman-Maze environment. As it can be seen, models without the memory module do not remember what it has generated before. This shows GameGAN opens up promising directions for not only game simulators, but as a general environment simulator that could mimic the real world.

5. Conclusion

We propose GameGAN which leverages adversarial training to learn to simulate games. GameGAN is trained by observing screenplay along with user's actions and does not require access to the game's logic or engine. GameGAN features a new memory module to ensure long-term consistency and is trained to separate static and dynamic elements. Thorough ablation studies showcase the modeling power of

GameGAN. In future works, we aim to extend our model to capture more complex real-world environments.

Acknowledgments

References

[1] Anonymous. Model based reinforcement learning for atari. In *Submitted to International Conference on Learning Representations*, 2020. under review. 3

[2] Randall D Beer and John C Gallagher. Evolving dynamical neural networks for adaptive behavior. *Adaptive behavior*, 1(1):91–122, 1992. 1

[3] Andrew Brock, Jeff Donahue, and Karen Simonyan. Large scale gan training for high fidelity natural image synthesis. *arXiv preprint arXiv:1809.11096*, 2018. 15

[4] Dian Chen, Brady Zhou, Vladlen Koltun, and Philipp Krhenbhl. Learning by cheating. In *Conference on Robot Learning (CoRL)*, pages 6059–6066, 2019. 1

[5] Xi Chen, Yan Duan, Rein Houthooft, John Schulman, Ilya Sutskever, and Pieter Abbeel. Infogan: Interpretable representation learning by information maximizing generative adversarial nets. In *Advances in neural information processing systems*, pages 2172–2180, 2016. 5, 15

[6] Silvia Chiappa, Sébastien Racaniere, Daan Wierstra, and Shakir Mohamed. Recurrent environment simulators. *arXiv preprint arXiv:1704.02254*, 2017. 2, 3, 6, 8

[7] Aidan Clark, Jeff Donahue, and Karen Simonyan. Efficient video generation on complex datasets. *arXiv preprint arXiv:1907.06571*, 2019. 2

[8] Emily Denton and Rob Fergus. Stochastic video generation with a learned prior. *arXiv preprint arXiv:1802.07687*, 2018. 2

[9] Emily L Denton and vighnesh Birodkar. Unsupervised learning of disentangled representations from video. In I. Guyon, U. V. Luxburg, S. Bengio, H. Wallach, R. Fergus, S. Vishwanathan, and R. Garnett, editors, *Advances in Neural Information Processing Systems 30*, pages 4414–4423. Curran Associates, Inc., 2017. 2

[10] Ian Goodfellow, Jean Pouget-Abadie, Mehdi Mirza, Bing Xu, David Warde-Farley, Sherjil Ozair, Aaron Courville, and Yoshua Bengio. Generative adversarial nets. In *Advances in neural information processing systems*, pages 2672–2680, 2014. 2, 15

[11] Alex Graves, Greg Wayne, and Ivo Danihelka. Neural turing machines. *arXiv preprint arXiv:1410.5401*, 2014. 4, 13

[12] Matthew Guzdial, Boyang Li, and Mark O Riedl. Game engine learning from video. In *IJCAI*, pages 3707–3713, 2017. 3

[13] David Ha and Jürgen Schmidhuber. Recurrent world models facilitate policy evolution. In *Advances in Neural Information Processing Systems*, pages 2450–2462, 2018. 2, 3, 6, 8

[14] Nikolaus Hansen and Andreas Ostermeier. Completely derandomized self-adaptation in evolution strategies. *Evolutionary computation*, 9(2):159–195, 2001. 8

[15] Sepp Hochreiter and Jürgen Schmidhuber. Long short-term memory. *Neural Comput.*, 9(8):1735–1780, Nov. 1997. 3

[16] Minyoung Huh, Shao-Hua Sun, and Ning Zhang. Feedback adversarial learning: Spatial feedback for improving generative adversarial networks. In *IEEE Conference on Computer Vision and Pattern Recognition*, 2019. 5

[17] Sergey Ioffe and Christian Szegedy. Batch normalization: Accelerating deep network training by reducing internal covariate shift. *arXiv preprint arXiv:1502.03167*, 2015. 15

[18] Phillip Isola, Jun-Yan Zhu, Tinghui Zhou, and Alexei A. Efros. Image-to-image translation with conditional adversarial networks. *CoRR*, abs/1611.07004, 2016. 2

[19] Ajay Jain, Sergio Casas, Renjie Liao, Yuwen Xiong, Song Feng, Sean Segal, and Raquel Urtasun. Discrete residual flow for probabilistic pedestrian behavior prediction. *arXiv preprint arXiv:1910.08041*, 2019. 1

[20] Michał Kempka, Marek Wydmuch, Grzegorz Runc, Jakub Toczek, and Wojciech Jaśkowski. Vizdoom: A doom-based ai research platform for visual reinforcement learning. In *2016 IEEE Conference on Computational Intelligence and Games (CIG)*, pages 1–8. IEEE, 2016. 2, 6

[21] Taeksoo Kim, Moonsu Cha, Hyunsoo Kim, Jung Kwon Lee, and Jiwon Kim. Learning to discover cross-domain relations with generative adversarial networks. In *Proceedings of the 34th International Conference on Machine Learning-Volume 70*, pages 1857–1865. JMLR. org, 2017. 2

[22] Diederik P Kingma and Jimmy Ba. Adam: A method for stochastic optimization. *arXiv preprint arXiv:1412.6980*, 2014. 16

[23] Anders Boesen Lindbo Larsen, Søren Kaae Sønderby, Hugo Larochelle, and Ole Winther. Autoencoding beyond pixels using a learned similarity metric. *arXiv preprint arXiv:1512.09300*, 2015. 3

[24] Alex X. Lee, Richard Zhang, Frederik Ebert, Pieter Abbeel, Chelsea Finn, and Sergey Levine. Stochastic adversarial video prediction. *CoRR*, abs/1804.01523, 2018. 2

[25] Ming-Yu Liu, Thomas Breuel, and Jan Kautz. Unsupervised image-to-image translation networks. *CoRR*, abs/1703.00848, 2017. 2

[26] Lars Mescheder, Andreas Geiger, and Sebastian Nowozin. Which training methods for gans do actually converge? *arXiv preprint arXiv:1801.04406*, 2018. 16

[27] Mehdi Mirza and Simon Osindero. Conditional generative adversarial nets. *arXiv preprint arXiv:1411.1784*, 2014. 5, 15

[28] Takeru Miyato and Masanori Koyama. cGANs with projection discriminator. In *International Conference on Learning Representations*, 2018. 2

[29] Volodymyr Mnih, Adria Puigdomenech Badia, Mehdi Mirza, Alex Graves, Timothy Lillicrap, Tim Harley, David Silver, and Koray Kavukcuoglu. Asynchronous methods for deep reinforcement learning. In *International conference on machine learning*, pages 1928–1937, 2016. 8

[30] Volodymyr Mnih, Koray Kavukcuoglu, David Silver, Alex Graves, Ioannis Antonoglou, Daan Wierstra, and Martin Riedmiller. Playing atari with deep reinforcement learning. *arXiv preprint arXiv:1312.5602*, 2013. 6

[31] Junhyuk Oh, Xiaoxiao Guo, Honglak Lee, Richard L Lewis, and Satinder Singh. Action-conditional video prediction using deep networks in atari games. In C. Cortes, N. D. Lawrence, D. D. Lee, M. Sugiyama, and R. Garnett, editors, *Advances in Neural Information Processing Systems 28*, pages 2863–2871. Curran Associates, Inc., 2015. 2

[32] Taesung Park, Ming-Yu Liu, Ting-Chun Wang, and Jun-Yan Zhu. Semantic image synthesis with spatially-adaptive normalization. In *Proceedings of the IEEE Conference on Computer Vision and Pattern Recognition*, pages 2337–2346, 2019. 2, 5, 14, 15

[33] Chris Paxton, Vasumathi Raman, Gregory D Hager, and Marin Kobilarov. Combining neural networks and tree search for task and motion planning in challenging environments. In *2017 IEEE/RSJ International Conference on Intelligent Robots and Systems (IROS)*, pages 6059–6066. IEEE, 2017. 1

[34] Scott E. Reed, Zeynep Akata, Xinchen Yan, Lajanugen Logeswaran, Bernt Schiele, and Honglak Lee. Generative adversarial text to image synthesis. In *Proceedings of the 33nd International Conference on Machine Learning, ICML 2016, New York City, NY, USA, June 19-24, 2016*, pages 1060–1069, 2016. 2

[35] Tim Salimans, Ian Goodfellow, Wojciech Zaremba, Vicki Cheung, Alec Radford, and Xi Chen. Improved techniques for training gans. In *Advances in neural information processing systems*, pages 2234–2242, 2016. 5, 15

[36] Nitish Srivastava, Elman Mansimov, and Ruslan Salakhudinov. Unsupervised learning of video representations using lstms. In *International conference on machine learning*, pages 843–852, 2015. 2

[37] Sergey Tulyakov, Ming-Yu Liu, Xiaodong Yang, and Jan Kautz. Mocogan: Decomposing motion and content for video generation. In *Proceedings of the IEEE conference on computer vision and pattern recognition*, pages 1526–1535, 2018. 2

[38] Dmitry Ulyanov, Andrea Vedaldi, and Victor Lempitsky. Instance normalization: The missing ingredient for fast stylization. *arXiv preprint arXiv:1607.08022*, 2016. 15

[39] Ting-Chun Wang, Ming-Yu Liu, Jun-Yan Zhu, Guilin Liu, Andrew Tao, Jan Kautz, and Bryan Catanzaro. Video-to-video synthesis. *CoRR*, abs/1808.06601, 2018. 2

[40] Dingdong Yang, Seunghoon Hong, Yunseok Jang, Tianchen Zhao, and Honglak Lee. Diversity-sensitive conditional generative adversarial networks. *arXiv preprint arXiv:1901.09024*, 2019. 5, 15

[41] Jun-Yan Zhu, Taesung Park, Phillip Isola, and Alexei A Efros. Unpaired image-to-image translation using cycle-consistent adversarial networks. In *Computer Vision (ICCV), 2017 IEEE International Conference on*, 2017. 2

Supplementary Material

We provide detailed descriptions of the model architecture (Section A), training scheme (Section B), and additional figures (Section C).

A. Model Architecture

We provide architecture details of each module described in Section 3. We adopt the following notation for describing modules:

Conv2D(a,b,c,d): 2D-Convolution layer with output channel size **a**, kernel size **b**, stride **c**, and padding size **d**.

Conv3D(a,b,c,d,e,f,g): 3D-Convolution layer with output channel size **a**, temporal kernel size **b**, spatial kernel size **c**, temporal stride **d**, spatial stride **e**, temporal padding size **f**, and spatial padding size **g**.

T.Conv2D(a,b,c,d,e): Transposed 2D-Convolution layer with output channel size **a**, kernel size **b**, stride **c**, padding size **d**, and output padding size **e**.

Linear(a): Linear layer with output size **a**.

Reshape(a): Reshapes the input tensor to output size **a**.

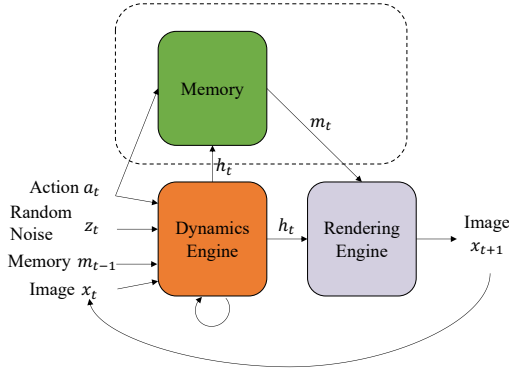**LeakyReLU(a):** Leaky ReLU function with slope **a**.

Figure 14: Overview of GameGAN: The *dynamics engine* takes a_t, z_t, and x_t as input to update the hidden state at time t. Optionally, it can write to and read from the external *memory module* (in the dashed box). Finally, the *rendering engine* is used to decode the output image x_{t+1}. The whole system is trained end-to-end. All modules are neural networks.

A.1. Dynamics Engine

The input action $a \sim \mathcal{A}$ is a one-hot encoded vector. For Pacman environment, we define $\mathcal{A} = \{left, right, up, down, stay\}$, and for the counterpart actions $\hat{a}$ (see Section 3.4.2), we define $\hat{left} = right$, $\hat{up} = down$, and vise versa. The images x have size $84 \times 84 \times 3$. For VizDoom, $\mathcal{A} = \{left, right, stay\}$, and $\hat{left} = right$, $\hat{right} = left$. The images x have size $64 \times 64 \times 3$.

At each time step t, a 32-dimensional stochastic variable z_t is sampled from the standard normal distribution $\mathcal{N}(0; I)$. Given the history of images $x_{1:t}$ along with a_t and z_t, GameGAN predicts the next image x_{t+1}.

For completeness, we restate the computation sequence of the dynamics engine (Section 3.1) here.

$$v_t = h_{t-1} \odot \mathcal{H}(a_t, z_t, m_{t-1}) \tag{12}$$

$$s_t = \mathcal{C}(x_t) \tag{13}$$

$$i_t = \sigma(W^{iv}v_t + W^{is}s_t), f_t = \sigma(W^{fv}v_t + W^{fs}s_t),$$
$$o_t = \sigma(W^{ov}v_t + W^{os}s_t) \tag{14}$$

$$c_t = f_t \odot c_{t-1} + i_t \odot \tanh(W^{cv}v_t + W^{cs}s_t) \tag{15}$$

$$h_t = o_t \odot \tanh(c_t) \tag{16}$$

where h_t, a_t, z_t, c_t, x_t are the hidden state, action, stochastic variable, cell state, image at time step t. $\odot$ denotes the hadamard product.

The hidden state of the dynamics engine is a 512-dimensional vector. Therefore, $h_t, o_t, c_t, f_t, i_t, o_t \in \mathbb{R}^{512}$.

$\mathcal{H}$ first computes embeddings for each input. Then it concatenates and passes them through two-layered MLP: [Linear(512),LeakyReLU(0.2),Linear(512)]. h_{t-1} can also go through a linear layer before the hadamard product in eq.13, if the size of hidden units differ from 512.

$\mathcal{C}$ is implemented as a 5 (for 64×64 images) or 6 (for 84×84 images) layered convolutional networks, followed by a linear layer:

Pacman	VizDoom
Conv2D(64, 3, 2, 0)	Conv2D(64, 4, 1, 1)
LeakyReLU(0.2)	LeakyReLU(0.2)
Conv2D(64, 3, 1, 0)	Conv2D(64, 3, 2, 0)
LeakyReLU(0.2)	LeakyReLU(0.2)
Conv2D(64, 3, 2, 0)	Conv2D(64,3, 2, 0)
LeakyReLU(0.2)	LeakyReLU(0.2)
Conv2D(64, 3, 1, 0)	Conv2D(64, 3, 2, 0)
LeakyReLU(0.2)	LeakyReLU(0.2)
Conv2D(64, 3, 2, 0)	Reshape(7*7*64)
LeakyReLU(0.2)	Linear(512)
Reshape(8*8*64)	
Linear(512)	

A.2. Memory Module

For completeness, we restate the computation sequence of the memory module (Section 3.2) here.

$$w = \text{softmax}(\mathcal{K}(a_t)) \in \mathbb{R}^{3\times3} \tag{17}$$

$$g = \mathcal{G}(h_t) \in \mathbb{R} \tag{18}$$

$$\alpha_t = g \cdot \text{Conv2D}(\alpha_{t-1}, w) + (1-g) \cdot \alpha_{t-1} \tag{19}$$

$$\mathcal{M} = \text{write}(\alpha_t, \mathcal{E}(h_t), \mathcal{M}) \tag{20}$$

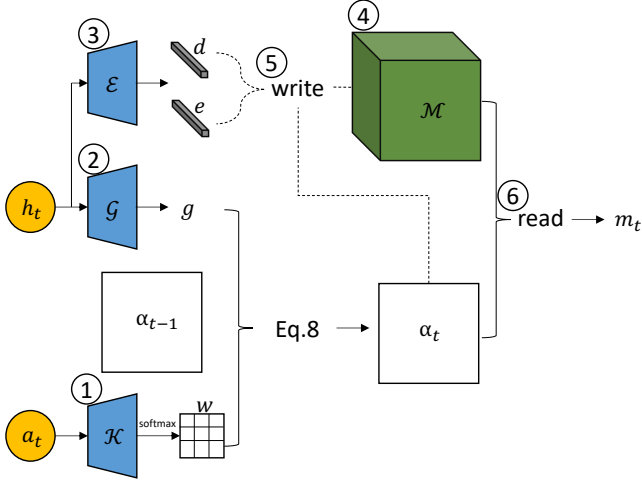$$m_t = \text{read}(\alpha_t, \mathcal{M}) \tag{21}$$

Figure 15: *Memory Module*. Descriptions for each numbered circle are provided in the text.

See Figure 15 for each numbered circle.

① $\mathcal{K}$ is a two-layered MLP that outputs a 9 dimensional vector which is softmaxed and reshaped to 3×3 kernel w: [Linear(512), LeakyReLU(0.2), Linear(9), Softmax(), Reshape(3,3)].

② $\mathcal{G}$ is a two-layered MLP that outputs a scalar value followed by the sigmoid activation function such that $g \in [0, 1]$: [Linear(512),LeakyReLU(0.2),Linear(1),Sigmoid()].

③ $\mathcal{E}$ is a one-layered MLP that produces an erase vector $e \in \mathbb{R}^{512}$ and an add vector $d \in \mathbb{R}^{512}$: [Linear(1024), split(512)], where Split(512) splits the 1024 dimensional vector into two 512 dimensional vectors. e additionally goes through the sigmoid activation function.

④ Each spatial location in the memory block $\mathcal{M}$ is initialized with 512 dimensional random noise $\sim N(0, I)$. For computational efficiency, we use the block width and height $N = 39$ for training and $N = 99$ for downstream tasks. Therefore, we use $39 \times 39 \times 512$ blocks for training, and $99 \times 99 \times 512$ blocks for experiments. Note that the shift-based memory module architecture allows any arbitrarily sized blocks to be used at test time.

⑤ write operation is implemented similar to the Neural Turing Machine [11]. For each location $\mathcal{M}^i$, write computes:

$$\mathcal{M}^i = \mathcal{M}^i(1 - \alpha_t^i \cdot e) + \alpha_t^i \cdot d \qquad (22)$$

where i denotes the spatial x, y coordinates of the block $\mathcal{M}$. e is a sigmoided vector which erases information from $\mathcal{M}^i$ when $e = \mathbf{1}$, and d writes new information to $\mathcal{M}^i$. Note that if the scalar α_t^i is 0 (*i.e.* the location is not being attended), the memory content $\mathcal{M}^i$ does not change.

⑥ read operation is defined as:

$$m_t = \sum_{i=0}^{N \times N} \alpha_t^i \cdot \mathcal{M}^i \qquad (23)$$

where $\mathcal{M}^i$ denotes the memory content at location i.

A.3. Rendering Engine

For the simple rendering engine of GameGAN -M, we first pass the hidden state h_t to a linear layer to make it a $7 \times 7 \times 512$ tensor, and pass it through 5 transposed convolution layers to produce the 3-channel output image x_{t+1}:

| Pacman	VizDoom
Linear(512*7*7)	Linear(512*7*7)
LeakyReLU(0.2)	LeakyReLU(0.2)
Reshape(7, 7, 512)	Reshape(7, 7, 512)
T.Conv2D(512, 3, 1, 0, 0)	T.Conv2D(512, 4, 1, 0, 0)
LeakyReLU(0.2)	LeakyReLU(0.2)
T.Conv2D(256, 3, 2, 0, 1)	T.Conv2D(256, 4, 1, 0, 0)
LeakyReLU(0.2)	LeakyReLU(0.2)
T.Conv2D(128, 4, 2, 0, 0)	T.Conv2D(128, 5, 2, 0, 0)
LeakyReLU(0.2)	LeakyReLU(0.2)
T.Conv2D(64, 4, 2, 0, 0)	T.Conv2D(64, 5, 2, 0, 0)
LeakyReLU(0.2)	LeakyReLU(0.2)
T.Conv2D(3, 3, 1, 0, 0)	T.Conv2D(3, 4, 1, 0, 0)
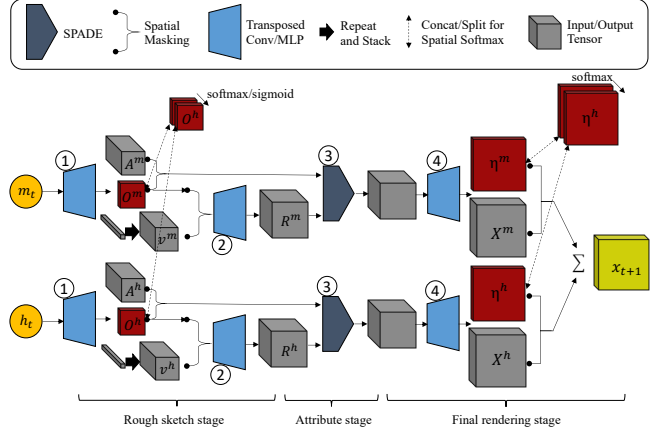
Figure 16: *Rendering engine* for disentangling static and dynamic components. Descriptions for each numbered circle are provided in the text.

For the specialized disentangling rendering engine that takes a list of vectors $\mathbf{c} = \{c^1, ..., c^K\} = \{m_h, h_t\}$ as input, the followings are implemented. See Figure 16 for each numbered circle.

① First, $A^k \in \mathbb{R}^{H_1 \times H_1 \times D_1}$ and $O^k \in \mathbb{R}^{H_1 \times H_1 \times 1}$ are obtained by passing c^k to a linear layer to make it a $3 \times 3 \times 128$ tensor, and the tensor is passed through two transposed convolution layers with filter sizes 3 to produce $\mathbb{R}^{7 \times 7 \times 32+1}$ tensor (hence, $H_1 = 7, D_1 = 32$):

Pacman & VizDoom
Linear(3*3*128)
Reshape(3,3,128)
LeakyReLU(0.2)
T.Conv2D(512, 3, 1, 0, 0)
LeakyReLU(0.2)
T.Conv2D(32+1, 3, 1, 0, 0)

Pacman	VizDoom
Conv2D(16, 5, 2, 0)	Conv2D(64, 4, 2, 0)
BatchNorm2D(16)	BatchNorm2D(64)
LeakyReLU(0.2)	LeakyReLU(0.2)
Conv2D(32, 5, 2, 0)	Conv2D(128, 3, 2, 0)
BatchNorm2D(32)	BatchNorm2D(128)
LeakyReLU(0.2)	LeakyReLU(0.2)
Conv2D(64, 3, 2, 0)	Conv2D(256, 3, 2, 0)
BatchNorm2D(64)	BatchNorm2D(256)
LeakyReLU(0.2)	LeakyReLU(0.2)
Conv2D(64, 3, 2, 0)	Conv2D(256, 3, 2, 0)
BatchNorm2D(64)	BatchNorm2D(256)
LeakyReLU(0.2)	LeakyReLU(0.2)
Reshape(3, 3, 64)	Reshape(3, 3, 256)

We split the resulting tensor channel-wise to get A^k and O^k. v^k is obtained from running c^k through one-layered MLP [Linear(32),LeakyReLU(0.2)] and stacking it across the spatial dimension to match the size of A^k.

② The rough sketch tensor R^k is obtained by passing v^k masked by O^k (which is either spatially softmaxed or sigmoided) through two transposed convolution layers:

Pacman	VizDoom
T.Conv2D(256, 3, 1, 0, 0)	T.Conv2D(256, 3, 1, 0, 0)
LeakyReLU(0.2)	LeakyReLU(0.2)
T.Conv2D(128, 3, 2, 0, 1)	T.Conv2D(128, 3, 2, 1, 0)

③ We follow the architecture of SPADE [32] with instance normalization as the normalization scheme. The attribute map A^k masked by O^k is used as the semantic map that produces the parameters of the SPADE layer, γ and β.

④ The normalized tensor goes through two transposed convolution layers:

Pacman	VizDoom
T.Conv2D(64, 4, 2, 0, 0)	T.Conv2D(64, 3, 2, 1, 0)
LeakyReLU(0.2)	LeakyReLU(0.2)
T.Conv2D(32, 4, 2, 0, 0)	T.Conv2D(32, 3, 2, 1, 0)
LeakyReLU(0.2)	LeakyReLU(0.2)

From the output tensor of the above, η^k is obtained with a single convolution layer [Conv2D(1, 3, 1)] and then is concatenated with other components for spatial softmax. We also experimented with concatenating η and passing them through couple of 1×1 convolution layers before the softmax, and did not observe much difference. Similarly, X^k is obtained with a single convolution layer [Conv2D(3, 3, 1)].

A.4. Discriminators

There are several discriminators used in GameGAN . For computational efficiency, we first get an encoding of each frame with a shared encoder:

Single Frame Discriminator   The job of the single frame discriminator is to judge if the given single frame is realistic or not. We use two simple networks for the patch-based (D_{patch}) and the full frame (D_{full}) discriminators:

D_{patch}	D_{full}
Conv2D(dim, 2, 1, 1)	Conv2D(dim, 2, 1, 0)
BatchNorm2D(dim)	BatchNorm2D(dim)
LeakyReLU(0.2)	LeakyReLU(0.2)
Conv2D(1, 1, 2, 1)	Conv2D(1, 1, 2, 1)

where dim is 64 for Pacman and 256 for VizDoom. D_{patch} gives 3×3 logits, and D_{full} gives a single logit.

Action-conditioned Discriminator   We give three pairs to the action-conditioned discriminator D_{action}: (x_t, x_{t+1}, a_t), $(x_t, x_{t+1}, \bar{a}_t)$ and $(\hat{x}_t, \hat{x}_{t+1}, a_t)$. x_t denotes the real image, $\hat{x}_t$ the generated image, and $\bar{a}_t \in \mathcal{A}$ a negative action which is sampled such that $\bar{a}_t \neq a_t$. The job of the discriminator is to judge if two frames are consistent with respect to the given action. First, we get an embedding vector for the one-hot encoded action through an embed-dinig layer [Linear(dim)], where $dim = 32$ for Pacman and $dim = 128$ for VizDoom. Then, two frames x_t, x_{t+1} are concatenated channel-wise and merged with a convolution layer [Conv2D(dim, 3, 1, 0), BatchNorm2D(dim), LeakyReLU(0.2), Reshape(dim)]. Finally, the action embedding and merged frame features are concatenated together and fed into [Linear(dim), BatchNorm1D(dim), LeakyReLU(0.2), Linear(1)], resulting in a single logit.

Temporal Discriminator   The temporal discriminator $D_{temporal}$ takes several frames as input and decides if they are a real or generated sequence. We implement a hierarchical temporal discriminator that outputs logits at several levels. The first level concatenates all frames in temporal dimension and does:
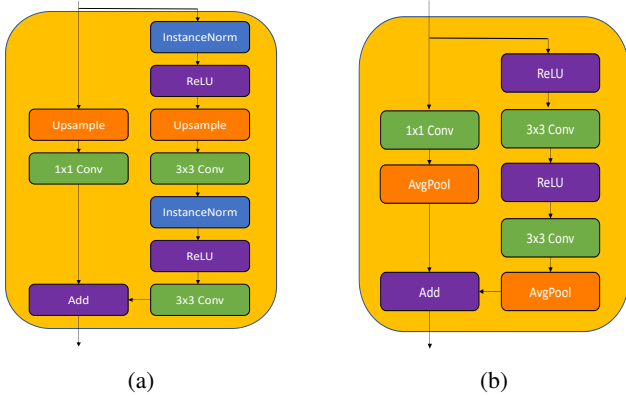
Figure 17: Residual blocks for the higher capacity model, modified and redrawn from Figure 15 of [3]. (a) A block for rendering engine, (b) A block for discriminator.

Conv3D(64, 2, 2, 1, 1, 0, 0)
BatchNorm3D(64)
LeakyReLU(0.2)
Conv3D(128, 2, 2, 1, 1, 0, 0)
BatchNorm3D(128)
LeakyReLU(0.2)

The output tensor from the above are fed into two branches. The first one is a single layer [Conv3D(1, 2, 1, 2, 1, 0, 0)] that produces a single logit. Hence, this logit effectively looks at 6 frames and judges if they are real or not. The second branch uses the tensor as an input to the next level:

Conv3D(256, 3, 1, 2, 1, 0, 0)
BatchNorm3D(256)
LeakyReLU(0.2)

Now, similarly, the output tensor is fed into two branches. The first one is a single layer [Conv3D(1, 2, 1, 1, 1, 0, 0)] producing a single logit that effectively looks at 18 frames. The second branch uses the tensor as an input to the next level:

Conv3D(512, 3, 1, 2, 1, 0, 0)
BatchNorm3D(512)
LeakyReLU(0.2)
Conv3D(1, 3, 1, 1, 1, 0, 0)

which gives a single logit that has an temporal receptive field size of 32 frames.

The Pacman environment uses two levels (up to 18 frames) and VizDoom uses all three levels.

A.5. Adding More Capacity

Both the rendering engine and discriminator described in A.3 and A.4 consist of only a few linear and convolutional layers which can limit GameGAN 's expressiveness. Motivated by recent advancements in image generation GANs [3, 32], we experiment with having higher capacity residual blocks. Here, we highlight key differences compared to the previous sections. The code will be released for reproducibility.

Rendering Engine: The convolutional layers in rendering engine are replaced by residual blocks described in Figure 17a. The residual blocks follow the design of [3] with the difference being that batch normalization layers [17] are replaced with instance normalization layers [38]. For the specialized rendering engine, having only two object types as in A.3 could also be a limiting factor. We can easily add more components by adding to the list of vectors (for example, let $\mathbf{c} = \{m_h, h_t^1, h_t^2, ...h_t^n\}$ where $h_t = concat(h_t^2, ...h_t^n)$) as the architecture is general to any number of components. However, this would result in $length(\mathbf{c})$ number of decoders. We relax the constraint for dynamic elements by letting $v^k = MLP(h_t) \in \mathbb{R}^{H_1 \times H_1 \times 32}$ rather than stacking v^k across the spatial dimension.

Discriminator: Increasing the capacity of rendering engine alone would not produce better quality images if the capacity of discriminators is not enough such that they can be easily fooled. We replace the shared encoder of discriminators with a stack of residual blocks shown in Figure 17b. Each frame fed through the new encoder results in a $N \times N \times D$ tensor where $N = 4$ for VizDoom and $N = 5$ for Pacman. The single frame discriminator is implemented as [Sum(N,N), Linear(1)] where Sum(N,N) sums over the $N \times N$ spatial dimension of the tensor. The action-conditioned and temporal discriminators use similar architectures as in A.4.

Figure 13 shows rollouts on Pacman trained with the higher capacity GameGAN model. It clearly shows that the higher capacity model can produce more realistic sharp images. Consequently, it would be more suitable for future works that involve simulating high fidelity real-world environments.

B. Training Scheme

We employ the standard GAN formulation [10] that plays a min-max game between the generator G (in our case, GameGAN) and the discriminators D. Let $\mathcal{L}_{\text{GAN}}$ be the sum of all GAN losses (we use equal weighting for single frame, action-conditioned, and temporal losses). Since conditional GAN architectures [27] are known for learning simplified distributions ignoring the latent code [40, 35], we add information regularization [5] $\mathcal{L}_{\text{Info}}$ that maximizes the mutual information $I(z_t, \phi(x_t, x_{t+1}))$ between the latent code z_t and the pair (x_t, x_{t+1}). To help the action-conditioned discriminator, we add a term that minimizes the cross entropy loss $\mathcal{L}_{\text{Action}}$ between a_t and $a_t^{pred} = \psi(x_{t+1}, x_t)$. Both ϕ and ψ are MLP that share lay-
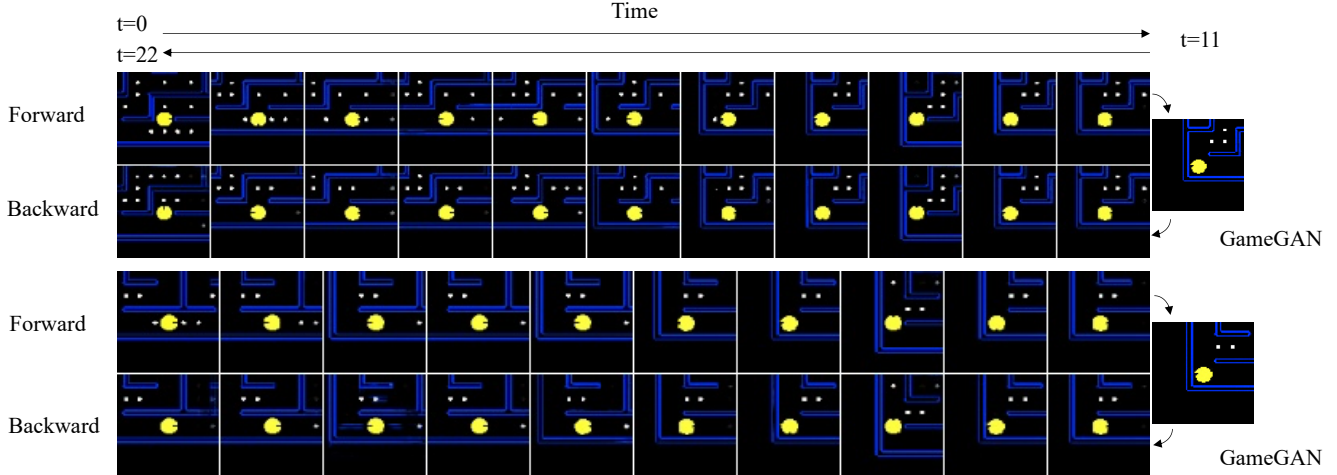
Figure 18: Additional Come-back-home task rollouts. The top row shows the forward path going from the initial position to the goal position. The bottom row shows the backward path coming back from the goal position to the initial position.
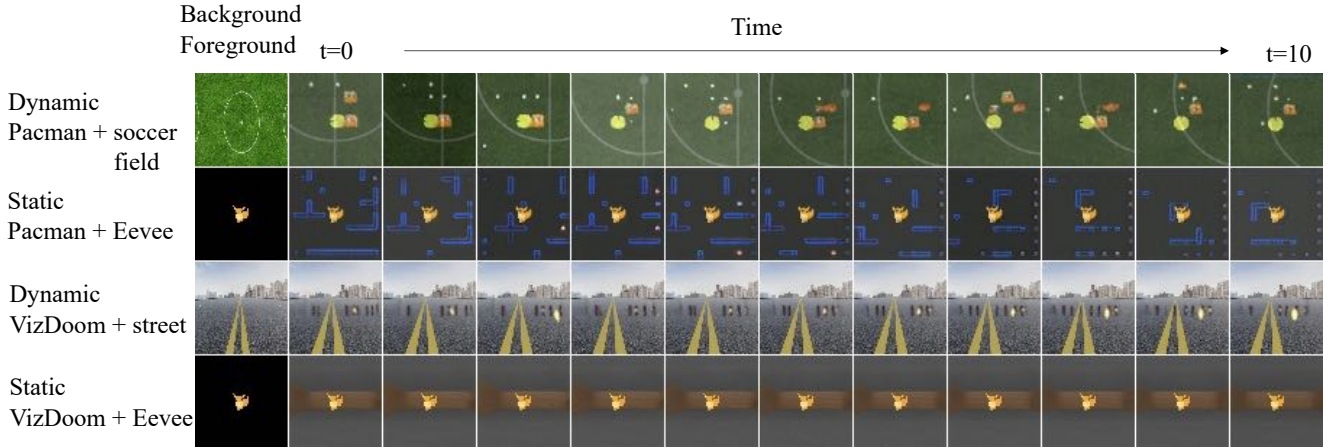

Figure 19: Additional rollouts of GameGAN by swapping background/foreground with random images.

ers with the action-conditioned discriminator except for the last layer. Lastly, we found adding a small L2 reconstruction losses in the image ($\mathcal{L}_{\text{recon}} = \frac{1}{T}\sum_{t=0}^{T}||x_t - \hat{x}_t||_2^2$) and feature spaces ($\mathcal{L}_{\text{feat}} = \frac{1}{T}\sum_{t=0}^{T}||feat_t - \hat{feat}_t||_2^2$) helps stabilize the training. x and $\hat{x}$ are the real and generated images, and $feat$ and $\hat{feat}$ are the real and generated features from the shared encoder of discriminators, respectively.

GameGAN optimizes:

$$\mathcal{L} = \mathcal{L}_{\text{GAN}} + \lambda_{\text{A}}\mathcal{L}_{\text{Action}} + \lambda_{\text{I}}\mathcal{L}_{\text{Info}} + \lambda_{\text{r}}\mathcal{L}_{\text{recon}} + \lambda_{\text{f}}\mathcal{L}_{\text{feat}} \tag{24}$$

When the memory module and the specialized rendering engine are used, $\lambda_{\text{c}}\mathcal{L}_{\text{cycle}}$ (Section 3.4.2) is added to $\mathcal{L}$ with $\lambda_{\text{c}} = 0.05$. We do not update the rendering engine with gradients from $\mathcal{L}_{\text{cycle}}$, as the purpose of employing $\mathcal{L}_{\text{cycle}}$ is to help train the dynamics engine and the memory module for long-term consistency. We set $\lambda_{\text{A}} = \lambda_{\text{I}} = 1$ and $\lambda_{\text{r}} = \lambda_{\text{f}} = 0.05$. The discriminators are updated after each optimization step of GameGAN . When traning the discriminators, we add a term γL_{GP} that penalizes the discriminator gradient on the true data distribution [26] with $\gamma = 10$.

We use Adam optimizer [22] with a learning rate of 0.0001 for both GameGAN and discriminators, and use a batch size of 12. GameGAN on Pacman and VizDoom environments are trained with a sequence of 18 and 32 frames, respectively. We employ a warm-up phase where 9 (for Pacman) / 16 (for VizDoom) real frames are fed into the dynamics engine in the first epoch, and linearly reduce the number of real frames to 1 by the 20-th epoch (the initial frame x_0 is always given).